

Alternating Parity Structures in $^{98,100,102}\text{Mo}$

S. Lalkovski¹, S. Ilieva^{1†}, A. Minkova¹, N. Minkov², T. Kutsarova²,
A. Lopez-Martens³, F. Hannachi³, A. Korichi³, H. Hübel⁴, A. Görgen^{4‡},
A. Jansen⁴, G. Schönwasser⁴, B. Herskind⁵, M. Bergström⁵, T. L. Khoo⁶,
D. Bazzacco⁷, and Zs. Podolyák^{8§}

¹ Department of Physics, University of Sofia, 1164 Sofia, Bulgaria

² Institute for Nuclear Research and Nuclear Energy, BAS, 1784 Sofia, Bulgaria

³ CSNSM Orsay, IN2P3/CNRS, F-91405, France

⁴ Helmholtz-Institut für Strahlen- und Kernphysik, Universität Bonn, Nussallee 14-16,
53115 Bonn, Germany

⁵ The Niels Bohr Institut, Blegdamsvej 17, DK-2100 Copenhagen, Denmark

⁶ Physics Division, Argonne National Laboratory, Argonne, Illinois 60439, USA

⁷ Dipartimento di Fisica e UNFN, Sezione di Padova, I-35131 Padova, Italy

⁸ INFN, Laboratori Nazionali di Legnaro, Italy

Abstract. Excited states in $^{98,100,102}\text{Mo}$ have been studied via the $^{30}\text{Si}+^{168}\text{Er}$ induced fission reaction at a beam energy of 142 MeV. Prompt γ -rays were detected with the EUROBALL IV multi-detector array. The level schemes are extended with more than 20 new transitions and interpreted in the framework of a soft-octupole vibration model.

1 Introduction

The appearance of octupole degrees of freedom in atomic nuclei is related to the coupling of two single particle orbitals with opposite parities and a difference of three units in the orbital and total angular momenta $\Delta l = \Delta j = 3$ [1]. Such pairs of orbitals are formed as a result of the odd-multipolarity octupole–octupole interaction between an intruder sub-shell (l, j) and a normal-parity sub-shell $(l-3, j-3)$ with a difference $\Delta N = 1$ in the major-shell quantum number N . They can be found in the valence shells of nuclei with more than 28 identical particles (neutrons or protons), where the spin-orbit coupling destroys the “normal” oscillator ordering of the levels. The octupole degrees of freedom are of considerable importance for the nuclear collective motion when the octupole correlated pair of orbitals is placed near the Fermi level. This situation is realized in several regions of the nuclear chart, such as the regions with identical particle number around 34, 56 and 88 where a strong $g_{9/2} - p_{3/2}$, $h_{11/2} - d_{5/2}$ and $i_{13/2} - f_{7/2}$ octupole coupling takes place, respectively [1].

From experimental point of view the fingerprints of octupole correlations in even-even nuclei can be found in the presence of low-lying 1^- and/or 3^- collective

[†] Present address: GSI, Darmstadt, Germany

[‡] Present address: DAPNIA/SPhN, CEA-Saclay, Gif-sur-Yvette, France

[§] Present address: Department of Physics, University of Surrey, Guildford, GU2 7XH, UK

states, in the observation of collective E3 transitions between the ground state and the lowest 3^- state, as well as in the presence of alternating parity energy sequences linked by enhanced E1 transitions [1]. The typical structure of an alternating parity band is observed in the region of light actinide nuclei Rn, Ra and Th [2–4]. In the low angular momenta $I < 7 - 8$ the negative parity levels appear above the neighboring even levels with energy $E_{1^-} > E_{2^+}$, $E_{3^-} > E_{4^+}$, and so on. At higher angular momenta $I > 8$ the parity shift effect rapidly decreases and a single octupole band with normally ordered levels is formed. This structure of the spectrum is related to the specific evolution of collectivity with the angular momentum [5].

In the region $A \approx 100$ a presence of low-lying octupole structure can be expected for the nucleus ^{98}Mo which has 56 neutrons. More generally the signature of octupole modes can be found in the existence of the low-lying 3^- and 5^- states and their γ decay patterns in the isotopes $^{98,100,102}\text{Mo}$. The parity shift effect, observed at the low angular momenta in these isotopes is similar in form, but stronger in magnitude than the effect observed in the region of light actinide nuclei.

The aim of the present work is to study the role of the octupole degrees of freedom in the nuclei $^{98,100,102}\text{Mo}$. The mass region around ^{98}Mo , where strongly pronounced octupole correlations are expected, is not well explored in terms of the collective approach, in contrast to the region of the light actinide nuclei Rn, Ra and Th [2]. We suggest that the stronger parity splitting observed in the octupole bands of $^{98,100,102}\text{Mo}$, compared to the light actinides, can be explained as the result of the respective larger octupole-softness. To analyze and interpret the excited states of these nuclei in the above aspect, we apply a collective model approach based on the presence of soft octupole degrees of freedom.

2 Experiment

Before our study, the low-lying excited states in ^{98}Mo were populated through β -decay and a number of reactions mainly with light particles [6] giving access to the low spin levels. The higher-lying yrast states in this nucleus were observed in $^{96}\text{Zr}(\alpha, 2n\gamma)$ [6] and $^{19}\text{F}+^{197}\text{Au}$ induced fission reaction [7]. In the present work we use $^{30}\text{Si}+^{168}\text{Er}$ induced fission reaction mechanism at beam energy 142 MeV which allows us to populate excited yrast states in $^{98,100,102}\text{Mo}$. The target thickness was 1.15 mg/cm^2 and it was set on 9 mg/cm^2 Au backing in order to stop the recoiling fragments. The complementary fragments of Mo nuclei are Zr isotopes, since no protons are evaporated during the fission process. The prompt γ -rays emitted from the excited nuclei were detected with the EUROBALL IV multidetector array [8] consisting of 30 single HpGe Compton-shielded detectors, 26 Clover and 15 Cluster composite Compton-shielded detectors. The experimental data were analyzed with RADWARE code package [9] and the preliminary results were reported in [10].

Table 1. γ -ray energies (in keV) and relative intensities in ^{98}Mo . The γ -ray energies are determined with an accuracy of 0.5 keV. The level energies are obtained from a least squares fit to γ -ray energies. Error bars are given in italic.

E_γ (keV)	I_γ	$I_i \rightarrow I_f$	E_i
334.5	5 2	(6+) \rightarrow (6+)	2678.9 7
385.1	6.4 <i>13</i>	(9-) \rightarrow (8+)	3657.1 7
394.2	9 4	(6, 7) \rightarrow (6+)	2738.7 8
416.8	2.8 4	(8+) \rightarrow (8+)	3271.9 7
431.5	6.9 <i>11</i>	(8, 9) \rightarrow (7-)	3527.9 8
475.3	16.4 <i>20</i>	(7-) \rightarrow (5-)	3096.6 7
510.7	24 3	(8+) \rightarrow (6+)	2854.8 7
560.2	9.3 <i>11</i>	(9-) \rightarrow (7-)	3657.1 7
603.1	7.8 <i>16</i>	(5-) \rightarrow 3-	2621.1 6
662.7	8.3 <i>10</i>	(10, 11) \rightarrow (8, 9)	4190.6 9
672.3	9.7 <i>13</i>	(9-) \rightarrow (7-)	3769.0 8
722.4	100	4+ \rightarrow 2+	1510.6 6
752.7	6.9 8	(7-) \rightarrow (6+)	3096.6 7
767.1	10.0 9	(11-) \rightarrow (9-)	4424.2 9
768.9	6.0 8	(11-) \rightarrow (9-)	4537.9 <i>10</i>
776.7	3.7 4	(13-) \rightarrow (11-)	5314.6 <i>11</i>
787.4	gate	2+ \rightarrow 0+	788.3 4
788.9	11.5 5	(8, 9) \rightarrow (6, 7)	3527.9 8
802.6	2.8 5	(9-) \rightarrow (8+)	3657.1 7
803.4	4.0 5	(12, 13) \rightarrow (10, 11)	4994.0 <i>11</i>
817.7	5.5 5	(15-) \rightarrow (13-)	6133.3 <i>11</i>
833.6	75 4	(6+) \rightarrow 4+	2344.2 6
877.6	12.0 <i>15</i>	(10+) \rightarrow (8+)	4149.6 8
878	-	(14+) \rightarrow (12+)	5925.4 <i>14</i>
891.4	4.6 5	(13-) \rightarrow (11-)	5315.6 <i>10</i>
897.8	5.5 5	(12+) \rightarrow (10+)	5047.4 9
927.9	21.2 <i>15</i>	(8+) \rightarrow (6+)	3271.9 7
1110.3	14.3 <i>13</i>	(5-) \rightarrow 4+	2621.1 6
1168.5	2.8 6	(6+) \rightarrow 4+	2678.9 7
1230.3	6.4 <i>14</i>	3- \rightarrow 2+	2018.0 4
1294.9	2.8 4	(10+) \rightarrow (8+)	4149.6 8
2017.3	3.7 9	3- \rightarrow 0+	2018.0 4

2.1 ^{98}Mo

The use of the high-efficient high-sensitive multidetector array gave the opportunity to confirm and extend the known level schemes of nuclei under study with more than 20 new transitions (Tables 1-3). Thus, the ground state band in ^{98}Mo (Figure 1) was extended with two transitions 898 and 878 keV up to (14+) level at 5925 keV energy. The negative-parity band, based on the 3- level at 2018 keV energy was extended up to the level at 5315 keV. A new structure, based on the known 2739 keV level was identified and extended up to 4994 keV level. The 432 keV transition links the

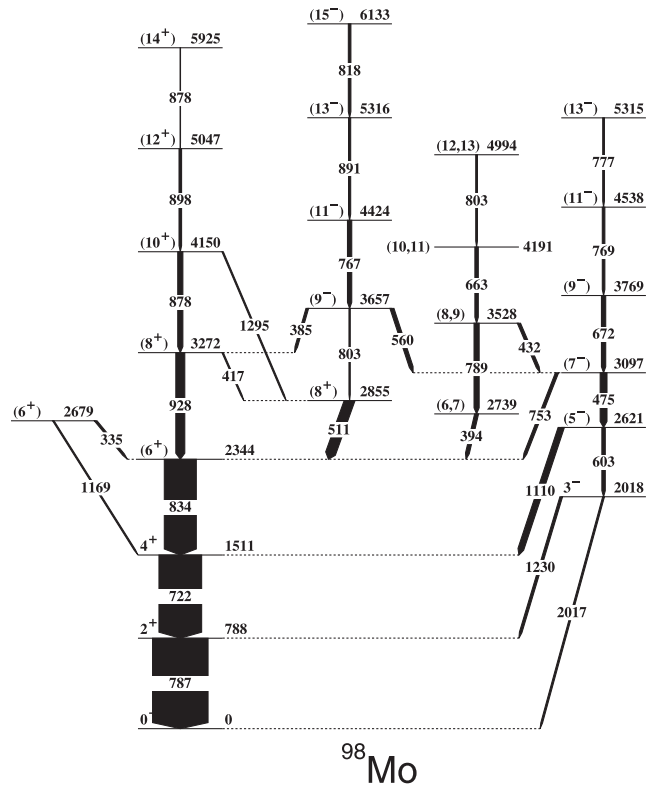


Figure 1. Excited states in ^{98}Mo . The arrow thickness is proportional to the relative γ -ray intensity.

new structure with the (7^-) state at 3097 keV. Another new structure, above the known 2855 keV level, was also observed for the first time here. It was extended up to 6133 keV level.

In general the spin and parity assignments in this work are based on the known adopted values [6, 11, 12]. The tentative spins and parities are assumed on the basis of the yrast γ -decay of nuclei, produced in induced fission reaction, on the γ -decay pattern of a particular level and on the observed band structure.

In particular, the spin-parity assignment of 2679 keV level (Figure 1) made in [6] is (4^+) . However, as commented in [6] it can also be 6^+ since in the (α, α') reaction the transferred angular momentum for the 2690 keV group is $6\hbar$. Here, tentatively assigned spin value $I=(6^+)$ is based on the observed decay pattern to 4^+ and (6^+) levels and on the fact that the $I=(4^+)$ state at the same energy would be strongly non-yrast. In spite of the observed relatively strong decay to (6^+) and 4^+ levels no populating transitions were found.

The 2855 keV and 3657 keV levels (Figure 1) are seen in $^{96}\text{Zr}(\alpha, 2n\gamma)$ reaction [13]). The spin value of the 2855 keV level assigned in [6] is $(6,7,8)$ and it

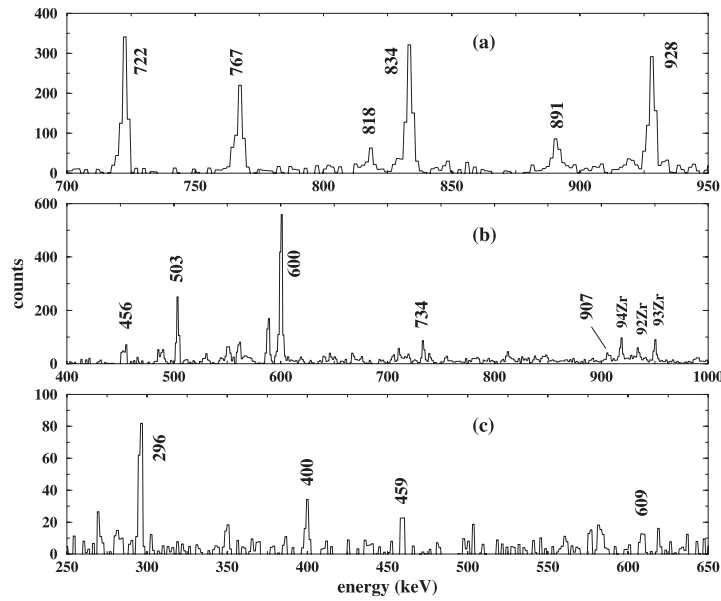


Figure 2. Coincidence spectra for: (a) ^{98}Mo , gated on 787/386; (b) ^{100}Mo , gated on 536/1204; (c) ^{102}Mo , gated on 447/1404.

is based on the observed γ decay to 6^+ level. The spin assignment (8^+) of the 2855 keV level, suggested here, is made on the basis of the observed 417 keV transition from (8^+) state and 1295 keV transition from (10^+) level. The spin value of the 3657 keV level (Figure 1) adopted in [6] is $I=(6^+, 7, 8, 9^-)$. Here, we made a tentative spin assignment on the basis of the γ -decay pattern to (7^-) and (8^+) states as well as on the assumption that it should be yrast state. The spin assignment of this level is also supported by the fact that there are no observed transitions to $I=(6^+)$ states.

The spin value of level 2739 keV adopted in [6] is $(6, 7, 8) \hbar$. Here, we suggest tentative $(6, 7)$ assignment since this level is weakly populated as compared to the other (8^+) levels.

Thus the level structures in ^{98}Mo reveal the following behaviour:

1. The yrast band shows near-vibrational behaviour since the energy of the states increases almost linearly with the spin. The disturbance of the vibrational structure at the beginning of the band can be caused by interaction between the two low-lying (6^+) state.
2. Below the (7^-) level at 3097 keV the positive and negative-parity quasi-bands are connected via 2017 keV E3 and 1230 keV, 1110 keV and 753 keV E1 transitions.

Above that level no linking E1 transitions have been found.

3. Below the (7^-) state at 3097 keV the negative-parity levels are shifted up with respect to their even-parity neighbours. After the (8^+) level a “normal” ordering of the levels takes place.
4. Above the (8^+) state at 2855 keV and (6,7) level at 2739 keV two new structures arise.

2.2 ^{100}Mo

The level scheme of ^{100}Mo was extended with 11 new transitions placed mainly in the two side bands (Figure 3 and Table 2). The band based on the (5^-) level at 2339 keV was extended up to 4940 keV. The new 432 keV transition de-excites the known (5^-) to the known 3^- level. We also observe the known from β -decay 544 keV transition in coincidence with a 683 keV transition. A new sequence of transitions: 641, 352, 944 keV has also been identified. Two new transitions at energies 371 keV and 589 keV feed and de-excite the new 2928 keV level.

Preliminary results on the study of the excited states in ^{100}Mo and ^{102}Mo nuclei were presented in [14]. The excited states reported there were populated in a different induced fission reaction $^{36}\text{S}+^{159}\text{Tb}$ at beam energy 165 MeV.

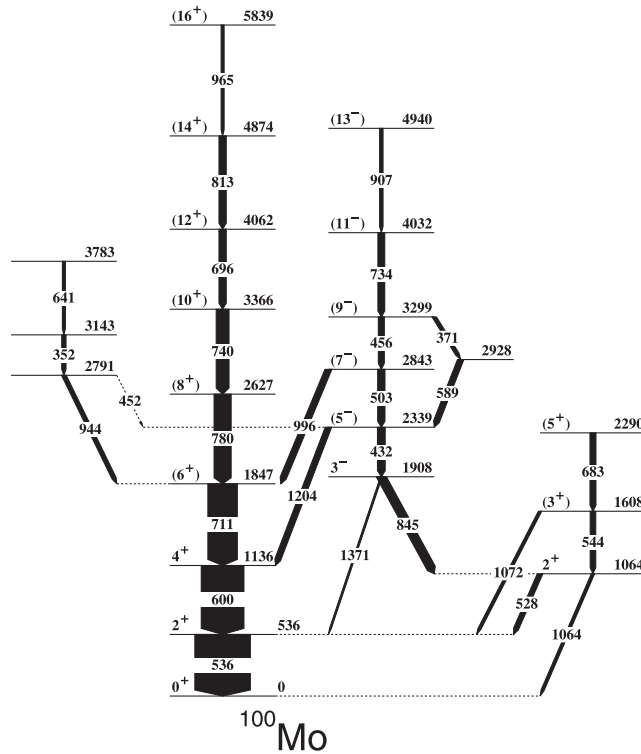


Figure 3. Excited states in ^{100}Mo . The arrow thickness is proportional to the γ -ray intensity.

Table 2. γ -ray energies (in keV) and relative intensities in ^{100}Mo . The γ -ray energies are determined with an accuracy of 0.5 keV. The level energies are obtained from a least squares fit to γ -ray energies. Error bars are given in italic.

E_γ (keV)	I_γ	$I_i \rightarrow I_f$	E_i
351.7	10.1 <i>24</i>		3142.5 <i>10</i>
370.5	9.1 <i>18</i>	$(9^-) \rightarrow (7^-)$	3298.9 <i>8</i>
431.5	17.6 <i>24</i>	$(5^-) \rightarrow (3^-)$	2339.4 <i>6</i>
456.1	13.7 <i>23</i>	$(9^-) \rightarrow (7^-)$	3298.9 <i>8</i>
503.2	16.8 <i>23</i>	$(7^-) \rightarrow (5^-)$	2842.8 <i>7</i>
528.4	12 <i>5</i>	$2^+ \rightarrow 2^+$	1063.7 <i>4</i>
535.6	gate	$2^+ \rightarrow 0^+$	535.7 <i>4</i>
544.1	13 <i>4</i>	$(3^+) \rightarrow 2^+$	1607.7 <i>5</i>
588.8	14.2 <i>25</i>	$(7^-) \rightarrow (5^-)$	2928.3 <i>7</i>
600.3	100	$4^+ \rightarrow 2^+$	1135.8 <i>6</i>
640.5	7.0 <i>15</i>		3783.0 <i>11</i>
682.5	14 <i>3</i>	$(5^+) \rightarrow (3^+)$	2290.2 <i>7</i>
695.5	17.0 <i>16</i>	$(12^+) \rightarrow (10^+)$	4061.8 <i>11</i>
711.1	69 <i>4</i>	$(6^+) \rightarrow 4^+$	1846.7 <i>7</i>
733.5	15.8 <i>21</i>	$(11^-) \rightarrow (9^-)$	4032.4 <i>9</i>
739.5	30.4 <i>22</i>	$(10^+) \rightarrow (8^+)$	3366.3 <i>10</i>
780.1	39.9 <i>25</i>	$(8^+) \rightarrow (6^+)$	2626.8 <i>9</i>
812.5	17.9 <i>15</i>	$(14^+) \rightarrow (12^+)$	4874.3 <i>12</i>
844.5	21 <i>3</i>	$3^- \rightarrow 2^+$	1907.8 <i>5</i>
907.1	7.9 <i>7</i>	$(13^-) \rightarrow (11^-)$	4939.5 <i>11</i>
944.1	10.0 <i>15</i>	$\rightarrow (6^+)$	2790.8 <i>9</i>
965 <i>1</i>	6.9 <i>23</i>	$(16^+) \rightarrow (14^+)$	5839.3 <i>16</i>
996.3	14.8 <i>14</i>	$(7^-) \rightarrow (6^+)$	2842.8 <i>7</i>
1064 <i>1</i>	7 <i>3</i>	$2^+ \rightarrow 0^+$	1063.7 <i>4</i>
1071.9	6.7 <i>21</i>	$(3^+) \rightarrow 2^+$	1607.7 <i>5</i>
1203.6	14.4 <i>15</i>	$(5^-) \rightarrow (4^+)$	2339.4 <i>6</i>
1371.4	4.1 <i>11</i>	$3^- \rightarrow 2^+$	1907.8 <i>5</i>

2.3 ^{102}Mo

The level scheme of ^{102}Mo , produced in the previous experiment [14] has also been confirmed and extended (Table 3). In addition to the level scheme reported in [15] we place a new transition of energy 400 keV depopulating the level (7^-) to (5^-) level. The (5^-) level is connected to the yrast band through the 1404 keV transition. The spin assignments are based again on the assumption that the spin should increase with the energy, on the observed band structure and on the systematics of the negative-parity bands in this region. Thus, on the contrary to stated in [15] spin values of the 2547, 3006, 3615 keV levels, we suggest the (7^-) , (9^-) , (11^-) spin assignments, respectively. Again, based on the assumption that the de excitation follows the yrast line we expect that the lowest possible spin value of the band head at 2459 keV is $6 \hbar$.

Table 3. γ -ray energies (in keV) and relative intensities in ^{102}Mo . The γ -ray energies are determined with an accuracy of 0.5 keV. The level energies are obtained from a least squares fit to γ -ray energies. Error bars are given in italic. With (a) are marked members of the yrast band; (b) members of the band, based on 2146.7 keV level; (c) members of the band, build on 2459.4 keV level.

E_γ (keV)	I_γ	$I_i \rightarrow I_f$	E_i
295.9 ^a	gate	$2^+ \rightarrow 0^+$	295.9 5
369.2 ^c	11.3 9	$(8^-) \rightarrow (6^-)$	2828.6 11
400.1 ^b	11.3 4	$(7^-) \rightarrow (5^-)$	2547.0 9
447.0 ^a	gate	$4^+ \rightarrow 2^+$	742.9 7
458.7 ^b	10.6 5	$(9^-) \rightarrow (7^-)$	3005.7 10
540.3 ^c	7.8 10	$(10^-) \rightarrow (8^-)$	3368.9 12
584.3 ^a	100	$6^+ \rightarrow 4^+$	1327.0 9
608.9 ^b	10.5 14	$(11^-) \rightarrow (9^-)$	3614.6 12
690.8 ^a	48.6 9	$8^+ \rightarrow 6^+$	2017.8 10
771.8 ^a	23.3 13	$10^+ \rightarrow 8^+$	2789.6 11
834.9 ^a	9.5 12	$(12^+) \rightarrow 10^+$	3624.5 12
1132.4	11.6 10	$(6^-) \rightarrow 6^+$	2459.4 10
1220.1	5.6 5	$(7^-) \rightarrow 6^+$	2547.0 9
1403.6	10.9 8	$(5^-) \rightarrow 4^+$	2146.7 9

In the present experiment ^{102}Mo is not so well populated as $^{98,100}\text{Mo}$ isotopes. The negative parity band, based on 2147 keV level is only extended up to angular momentum $11\hbar$. It has to be noted that a 3^- level is not observed in the present experiment, which might be due to the fact that it is strongly non yrast. For the purpose of the discussion we shall use the adopted 3^- level at 1881 keV energy seen only in a (d,p) reaction [12].

3 Discussion

In the considered $^{98,100,102}\text{Mo}$ isotopes the negative-parity levels with $I^\pi = 3^-$ and 5^- are shifted up with respect to the 4^+ and 6^+ states. The observed parity shift effect is similar in form and larger in magnitude, compared to the splitting observed in the region of light actinides. Further, with the increase of the angular momentum, a normal ordering of the energy levels takes place. From the collective point of view the following physical interpretation of the observed phenomenon can be given. In the nuclei with strong octupole correlations the collective potential has two minima located at positive and negative values of the octupole deformation parameter β_3 . The parity shift effect in the collective energy levels is due to the tunneling of the shape between the two minima through the potential barrier separating them. The decrease in the parity shift with the angular momentum is related to the respective decrease in the tunneling probability as a result of an increase in the barrier height [5]. On the other hand, the intrinsic degrees of freedom can essentially influence the collective band structure by causing a sign inversion in the

parity shift [16]. At certain critical frequency the Coriolis force can destroy a pair of particles trying to align their angular momenta along the collective rotation. Then the single-particle momenta give an essential contribution to the total angular momentum. The collective angular momentum decreases respectively, which leads to a decrease in the potential barrier. Thus, the pair-breaking process causes a local increase in the penetration probability and a respective increase in the parity shift effect [16]. At the same time, if the separated particles (after the breaking) occupy orbitals with opposite parity, the parity π_{sp} of the single-particle wave function will change in sign. This will entail an inversion in the parity π_{oct} of the octupole potential wave function and subsequently, an inversion in the sign of the parity shift effect. Actually, the ‘‘total parity’’ π is related to the octupole and the single particle parities as $\pi = \pi_{oct} \cdot \pi_{sp}$.

The above considered collective dynamics is observed in ^{98}Mo (with a sign inversion effect) and in $^{100,102}\text{Mo}$ (without sign inversion). To analyze the structure of alternating parity bands in these nuclei, we apply a collective model with soft octupole degrees of freedom [17]. This model is based on a Hamiltonian describing the collective motion of a system with respect to the octupole-deformation variable β_3

$$H_{vib}^{oct} = -\frac{\hbar^2}{2B_3} \frac{d^2}{d\beta_3^2} + U_I(\beta_3). \quad (1)$$

The octupole potential is taken in the form of an angular momentum dependent symmetric double-well with minima fixed at some value $\beta_{3\min}$ of the octupole deformation

$$U_I(\beta_3) = \frac{(\beta_3^2 - \beta_{3\min}^2)^2 I(I+1) d_2^2}{2(d_1 + d_2 \beta_{3\min}^2)^2 (d_1 + d_2 \beta_3^2)}. \quad (2)$$

B_3 is an effective octupole mass parameter, while d_1 and d_2 have the meaning of inertial parameters. The model energy levels are given by the equation

$$E(I) = E_0 + \frac{1}{2} (1 + \pi(-1)^I) E^{(\pi_{oct})}(I), \quad (3)$$

where the octupole parity $\pi_{oct} = \pm$ is determined by the total and the single-particle parities as $\pi_{oct} = \pi \cdot \pi_{sp}$. $E^{(\pi_{oct})}$ is one of the octupole-vibration energy levels $E^{(+)}$ or $E^{(-)}$ obtained by solving numerically the Schrödinger equation for the Hamiltonian (1) with the potential (2). $E^{(+)}$ is the lowest level in the potential (2) and has positive parity $\pi_{oct} = (+)$, while $E^{(-)}$ is the next (higher) level which has a negative parity $\pi_{oct} = (-)$ (for more details see [17]). The second term in Eq. (3) switches between $E^{(+)}$ and $E^{(-)}$ in dependence on the sign of the total parity π , as well as on the sign of the single particle parity π_{sp} . In the low angular momentum region π_{sp} is positive. Then according to Eq. (3) the states with positive total parity π correspond to $E^{(+)}$, while the states with negative total parity correspond to $E^{(-)}$. As a result the negative (total) parity levels are shifted up with respect to the positive ones. When π_{sp} becomes negative (after a pair-breaking process) the states with positive π correspond to $E^{(-)}$ while the ones with negative π correspond to $E^{(+)}$.

Then the positive parity levels are shifted up and the sign of the parity splitting is inverted. The quantity E_0 determines the origin of the energy scale of the spectrum.

The model energy levels for the nuclei $^{98,100,102}\text{Mo}$ are obtained by Eq. (3) after adjusting the Hamiltonian parameters with respect to the experimental energy levels of each nucleus. The obtained parameter values are given in Table 4. In ^{98}Mo a change of π_{sp} from positive at $I < 8$ to negative at $I \geq 9$ is assumed on the basis of the sign inversion of the experimentally observed parity shift. In ^{102}Mo an additional parameter $d_0 = 50\hbar^2$ is superposed to the term $I(I + 1)$ in the potential (2) in order to describe the sharp exponential decrease in the parity shift at the lowest angular momentum levels. (More details on the meaning of d_0 are given in Section 4 of [17].)

The theoretical and experimental energies are compared in (Table 5). The result allows us to analyze the evolution of the spectrum with the angular momentum for each isotope. Thus we can examine the behaviour of the odd-even energy displacement ($\Delta I = 1$ staggering) measured by the five-point staggering formula

Table 4. Parameter values for the model fits of energy levels in $^{98,100,102}\text{Mo}$.

Nucl.	E_0 keV	d_1 \hbar^2/MeV	d_2 \hbar^2/MeV	b_{3min} dim.less	B_3 \hbar^2/MeV
^{98}Mo	301.4	0.028	0.146	0.118	70
^{100}Mo	160.2	0.026	0.129	0.109	70
^{102}Mo	-1767	0.004	0.013	0.080	90

Table 5. Theoretical and experimental energies in keV in ^{98}Mo and ^{100}Mo .

I [\hbar]	^{98}Mo		^{100}Mo		^{102}Mo	
	Eth	Eexp	Eth	Eexp	Eth	Eexp
1 ⁻	1260	–	1135	–	1538	–
2 ⁺	852	787	648	536	395	296
3 ⁻	1921	2018	1786	1908	1749	1881
4 ⁺	1497	1511	1136	1136	766	743
5 ⁻	2524	2621	2323	2339	2099	2147
6 ⁺	2327	2344	1785	1847	1312	1327
7 ⁻	3178	3097	2870	2843	2554	2547
8 ⁺	3222	3272	2544	2627	1990	2018
9 ⁻	3887	3769	3457	3299	3096	3006
10 ⁺	4258	4150	3349	3366	2756	2790
11 ⁻	4529	4538	4084	4032	3708	3615
12 ⁺	5022	5047	4151	4062	3570	3625
13 ⁻	5362	5315	4744	4940	4374	–
14 ⁺	5804	5925	4931	4874	4403	–
15 ⁻	6177	–	5427	–	–	–
16 ⁺	6594	–	5690	5839	–	–

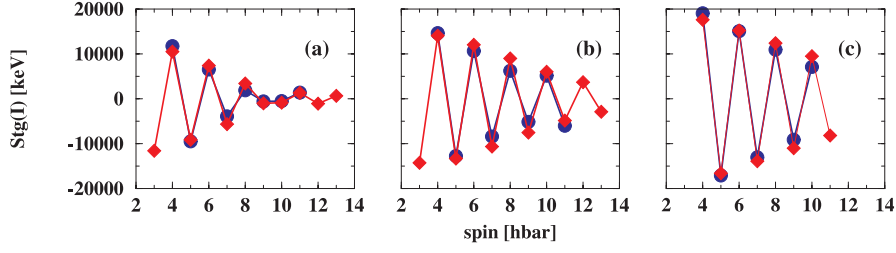


Figure 4. Experimental (circles) and theoretical (diamonds) staggering plots for ^{98}Mo (a), ^{100}Mo (b) and ^{102}Mo (c). The same energy scale is used for all the isotopes.

$$\text{Stg}(I) = 6\Delta E(I) - 4\Delta E(I-1) - 4\Delta E(I+1) + \Delta E(I+2) + \Delta E(I-2) \quad (4)$$

The experimental and theoretical staggering patterns for the nuclei $^{98,100,102}\text{Mo}$ are compared in Figure 4. It is seen that the magnitude of the staggering increases from ^{98}Mo to ^{102}Mo . Also, we see that the odd-even staggering in the considered Mo isotopes is larger with about an order in magnitude than the staggering observed in the region of light actinides [17]. This observation provides a quantitative estimation for the difference in the octupole softness of the collective potential in both regions.

On the other hand, in each of the considered nuclei the staggering amplitude decreases with the increasing angular momentum. As has been discussed above, this is related to the decreasing tunneling effect and the respective stabilization of the octupole shape towards higher angular momenta. In ^{98}Mo the staggering exhibits faster decrease compared to ^{100}Mo and ^{102}Mo showing better development of the octupole collectivity in this nucleus.

In addition, in ^{98}Mo the experimental odd-even staggering shows an irregularity in the region $I \sim 10$ with an inversion in the phase of oscillations. As it was mentioned above, this effect can be considered as an indication for the change of the single particle parity π_{sp} . The analysis of the staggering quantity (4) suggests that π_{sp} changes from (+) to (-) for $I \geq 9$. This effect can be related to the presence of a pair breaking process, which in this mass region arises from $\nu h_{11/2}$. Thus, the decrease of the octupole potential barrier in ^{98}Mo can be caused by the $\nu h_{11/2}$ pair breaking. Further, the sign inversion of the parity shift suggests that after the breaking both particles occupy orbitals with opposite parity, such as $\nu h_{11/2}$ and $d_{5/2}$ or $\nu g_{7/2}$.

In conclusion, the present work provides extended level schemes of $^{98,100,102}\text{Mo}$ nuclei produced in induced fission reaction. The level schemes of ^{98}Mo and ^{100}Mo were extended with 11 new transitions in each nucleus. 16 new levels were found in these nuclei. Two new transitions, feeding and de-exciting the new 2147 keV level, were found in ^{102}Mo . New spin and parity assignments of 25 levels in $^{98,100,102}\text{Mo}$ were also made. So far obtained new level information reveal the possibility to study the evolution of the staggering pattern with the change in neutron number. It was shown that the magnitude of the observed odd-even staggering effect increases with

the increasing neutron number and can be associated with the increase of the octupole softness from ^{98}Mo to ^{102}Mo . On the other side, the sign inversion effect observed in the staggering pattern of ^{98}Mo indicates the influence of the intrinsic (single particle) degrees of freedom on the octupole collectivity. It can be concluded that the octupole degrees of freedom are of essential importance for the collective properties of nuclei in the region of ^{98}Mo .

Acknowledgments

S.L. acknowledges valuable discussions with Prof. P. von Brentano and Dr. P. Petkov.

The work is supported by the Bulgarian National Science fund under contracts F-1502/05 and MU-405/05 and by BMBF under contract 06 BN 109.

References

1. P.A. Butler and W. Nazarewicz, *Rev. Mod. Phys.* **68**, 349 (1996); S.G. Rohozinski, *Rep. Prog. Phys.* **51**, 541 (1988).
2. J.F.C. Cocks *et al.*, *Phys. Rev. Lett.* **78**, 2920 (1997).
3. A. Artna-Cohen, *Nucl. Data Sheets* **80**, 227 (1997).
4. Y.A. Akovali, *Nucl. Data Sheets* **77**, 433 (1996).
5. R. Jolos, P. von Brentano, F. Döna, *J. Phys. G* **19**, L151 (1993).
6. B. Singh and Z. Hu, *Nucl. Data Sheets* **98**, 335 (2003).
7. Y. Abdelrahman, J.L. Durell, W. Gelletly, W.R. Phillips, I. Ahmad, R. Holzmann, R.V.F. Janssens, T.L. Khoo, W.C. Ma, M.W. Drigert, *Phys. Lett. B* **199**, 504 (1987).
8. J. Simpson, *Z. Phys. A* **358**, 139 (1997).
9. D. C. Radford, *Nucl. Instrum. Methods Phys. Res. A* **361**, 297 (1995).
10. S. Lalkovski, S. Ilieva, A. Minkova, A. Lopez-Martens, F. Hannachi, A. Korichi, T. Kutsarova, N. Minkov, *BgNS Transactions* **10**, 311 (2005), Proc. from the *XVI International school on nuclear physics, neutron physics and nuclear energy* (2005) Varna, Bulgaria.
11. B. Singh, *Nucl. Data Sheets* **81**, 1 (1997).
12. D. de Frenne and E. Jacobs, *Nucl. Data Sheets* **83**, 535 (1998).
13. C.M. Lederer, J.M. Jaklevic, J.M. Hollander, *Nucl. Phys. A* **169**, 449 (1971).
14. S. Ilieva, S. Lalkovski, D. L. Balabanski, M. Danchev, L. L. Riedinger, *Prog. Rep. on Nuclear Spectroscopic Studies*, ed. by C.R. Bingham and L.L. Riedinger, p. 10, Knoxville, 2004.
15. H. Hua *et al.*, *Phys. Rev. C* **69**, 014317 (2004).
16. R.V. Jolos and P. von Brentano, *Phys. Rev. C* **60**, 064317 (1999); R.V. Jolos, N. Minkov, W. Scheid, *Phys. Rev. C* **72**, 064312 (2005).
17. N. Minkov, P. Yotov, S. Drenska, W. Scheid, *J. Phys. G* **32**, 497 (2006).